The 6th IASPEI / IAEE International Symposium: Effects of Surface Geology on Seismic Motion
August 2021

SUITABILITY OF THE 1D ASSUMPTION FOR GROUND RESPONSE ANALYSIS IN THE EPICENTRAL AREA OF THE 2016 Mw 6.0 AMATRICE EARTHQUAKE (CENTRAL ITALY)

Hailemikael Salomon[1], Di Giulio Giuseppe[2], Felicetta Chiara[2], Mascandola Claudia[2], Pacor Francesca[2] and Spallarossa Daniele[3]
1 Researcher, ENEA, Frascati, Italy (salomon.hailemikael@enea.it)
2 Researcher, Istituto Nazionale di Geofisica e Vulcanologia, Italy (chiara.felicetta@ingv.it; giuseppe.digiulio@ingv.it; francesca.pacor@ingv.it; claudia.mascandola@ingv.it)
3 Professor of Geophysics, Università degli Studi di Genova, Genova, Italy (daniele@dipteris.unige.it)

ABSTRACT

The 2016-2017 Central Italy seismic sequence was recorded by the 3A network deployed in the epicentral area and composed of 50 seismic stations. Taking advantage of microzonation activities, we retrieved site information for a subset of these stations, including shear-wave velocity profiles from down-hole tests down to a minimum depth of 30 m. In this paper we compared the available empirical transfer functions with the theoretical one-dimensional transfer functions calculated from site characterization information. The former were computed by weak-motions spectral ratios using either a reference site (SSR) or horizontal-to-vertical ratios (EHV); the theoretical curves were computed using the STRATA code under the linear-elastic assumption. We have applied some classification strategies to discriminate sites that can be interpreted as having a 1D site response. We observed a poor match between empirical and theoretical amplification functions, suggesting that the 1D assumption may not hold for the majority of the selected stations.

Keywords: seismic motion, site effect, empirical amplification functions, 1D modeling, 2016 Amatrice earthquake.

INTRODUCTION

Site effects are usually estimated through numerical modeling based on the subsurface characterization obtained by geophysical and geological surveys. The field surveys are useful to define near-surface velocity profiles that are subsequently used in the simulation codes usually adopted in the engineering-seismology community. In particular, seismic microzonation studies rely on computed site response , and the current practice, at least during the initial levels of the microzonation study, is to perform one-dimensional (1D) simulations for SH waves. It is therefore important to investigate the reliability of the 1D assumptions, and to quantify the uncertainty between predicted and observed local amplifications. To this aim, we take advantage of the experimental transfer functions and site characterization information available for a temporary seismic network (code 3A; http://terremoti.ingv.it/en/instruments/network/3A) that was installed in the area struck by the 2016-2017 Central Italy seismic sequence (Cara et al. 2019). 3A network was operating for seismic microzonation purposes between September and November 2016 and recorded part of the seismic sequence started on August 24th, 2016, with the Mw 6.0 Amatrice mainshock. Both velocimetric and accelerometric sensors were installed in 50 sites (Fig. 1), encompassing an area characterized by complex geological settings (morphological terraces, river valleys, steep slopes) in the Amatrice and Accumoli municipalities. The 3A network recorded a large number of events in a wide range of magnitudes, including, only for a few stations, also the Mw 5.9 and 6.5 events of October 26th and 30th, respectively. For about half of the recording stations, information about site conditions at the near-surface were obtained by geological and geophysical surveys performed in the proximity of each station (at distance within 100 m) for the seismic microzonation activity. Such data include stratigraphic log, geomorphological setting, single-station noise measurement and S-wave velocity profile derived both from passive array (active and passive masw) and shallow downhole tests

(maximum depth of investigation < 50 m). Fig. 2 groups the shear-wave velocity (Vs) profiles obtained from these tests according to different geological conditions: sites located on geological bedrock, sites characterized by shallow deposits (within 10 m thickness) overlaying the geological bedrock and sites settled on relatively thick alluvial terraces. As reported in a recent paper (Felicetta et al. 2021), the empirical amplification functions were computed at each stations of the 3A network using Standard Spectral Ratio (SSR) and Horizontal-to-Vertical Spectral Ratio methods, with the latter applied both to earthquake (EHV) and noise recordings (HVSR). These results showed that amplification is found mostly at intermediate frequencies (2-5Hz) and that a vertical amplification is also present in many sites. The spatial distribution of ground-motion amplification is related with the local geological conditions, which are supposed to be fairly well known for the shallower 50 m. In the same paper by Felicetta et al. 2021, a cluster analysis has been applied to find the natural aggregation of the empirical site amplification, founding five and three main groups of sites with a different trend of the amplification curves in the horizontal and vertical components, respectively.
In the present work we compared the SSR and EHV empirical functions to the theoretical 1D transfer functions computed using the STRATA software. We applied some classification strategies proposed in literature (Thompson et al. 2012; Tao and Rathje 2020) for discriminating sites that can be interpreted as having a 1D seismic site response. In the majority of sites, we obtained a poor fit between empirical transfer functions (ETF) and theoretical amplification functions (TTF), suggesting that the knowledge of the shallower subsurface (< 50 m) and the 1D wave propagation assumption are not very suitable for the evaluation of site response in such complex geological settings.

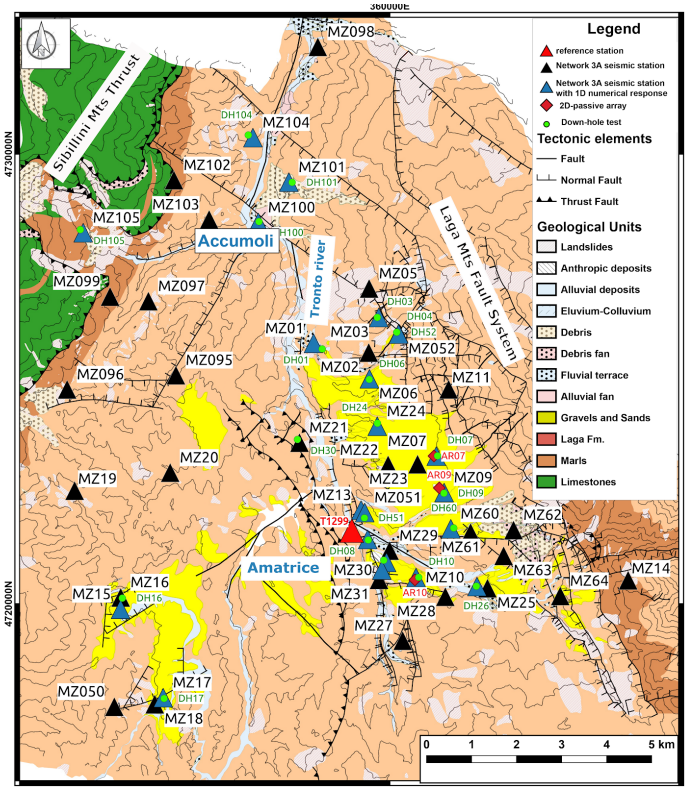

Figure 1. Geological sketch of the studied area. The triangles show the position of the 3A stations.

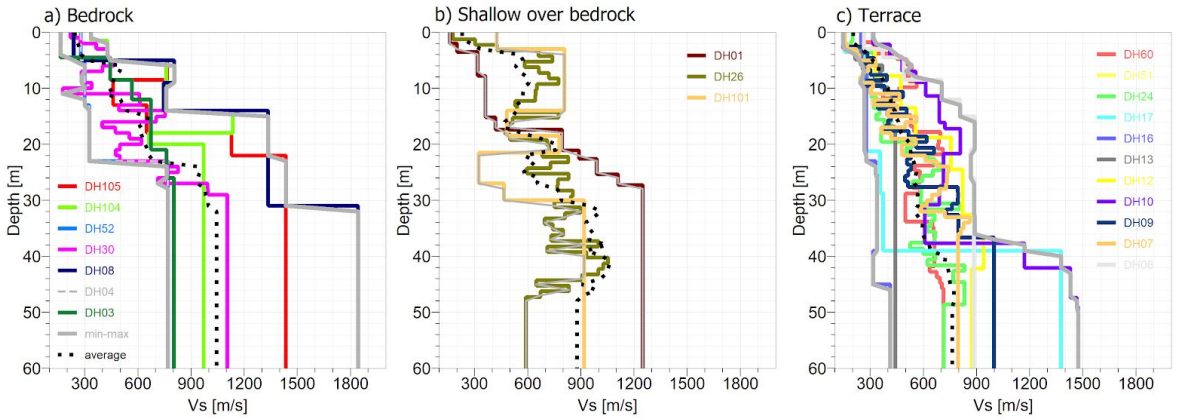

Figure 2. Shear-wave velocity (Vs) profiles obtained from downhole and geophysical tests at the stations of the 3A network. Vs profiles are grouped by geological setting: outcropping geological bedrock sites (left panel), shallow deposits overlying bedrock (middle panel) and alluvial terrace sites (right panel). The dashed profile indicates the averaged traveltime.

Analysis and Methods

SSR and 1D theoretical transfer function

The spectral ratio analysis was based on a bulletin with 615 events in the magnitude range 3-5 and epicentral distance 0-60 km from the Amatrice village (Fig. 1). SSRs and EHVs were computed on a time window of 6sec length starting from the S-wave arrival, and the station T1299 has been used as a reference site for the SSR calculations (see Fig. 1) consistently with the previous studies on local effects in the Amatrice area (Milana et al. 2019). Details on the analysis and results at all the stations are reported in Felicetta et al., 2021. Data from geophysical and geological surveys allowed us to define a 1D subsoil model at the near-surface (depth < 100 m) for 24 sites of the 3A network (Fig. 2). These models were mostly obtained by specific downhole and surface-wave array experiments carried out within a maximum distance of 100 m from the station. After defining the stratigraphic and Vs models, the theoretical transfer functions were computed by a 1D convolution approach using the STRATA software (Kottke and Rathje 2009), which is able to perform linear-elastic and equivalent-linear site response analyses. As the empirical site amplification functions were estimated on the basis of a dataset mainly made of weak-motion records, we run STRATA simulations using the linear-elastic approach. STRATA allows for stochastic variation of the site properties, including the Vs values, layer thicknesses, depth to bedrock, shear-modulus reduction (G/G0) and material damping (D) curves. As input motion at the bedrock level, we used 7 strong-motion data compliant with the 475 years return period of uniform hazard spectrum of the Italian seismic code (Luzi et al., 2020). The input motions, which include records of the 2016 seismic sequence (4 records of the Mw 6.5 on October 30; 3 records of the Mw 5.9 event on October 26), were applied at the bedrock level assuming an elastic boundary condition. The bedrock level was defined as having a Vs equal or larger than 800 m/s. The G/G0 and D data were selected from literature, or from the laboratory surveys performed on few subsoil samples collected in the epicentral area (reference EmerTer Project Working Group, 2018). For each of the selected sites, the transfer function (the ratio between the outcrop and the bedrock level) was computed averaging 200 STRATA simulations in the linear-elastic case, obtained varying the velocity of each layer into the selected profile. The Vs values were varied following the statistical models by Toro (1995), within a range ±20% of the Vs value inferred by downhole or array surveys to take into account possible uncertainties on velocities. In case the seismic bedrock level was not reached in the Vs profile, the depth-to-bedrock was also varied between 50 and 200 m depth using a uniform distribution and assuming an average Vs of 1250 m/s. One correlation model was set for all

sites of EC8 classes B and C, corresponding to the EC8-B class because the majority of the stations of the network 3A falls in this category and several EC8-C class sites present time-averaged shear-wave velocity for the shallower 30 m (V_{S30}) very close to the lower bound of site class B, whereas the EC8-E correlation model was used for those sites in the corresponding class. The 1D theoretical transfer functions (TTF) were computed by STRATA as the ratio between the Fourier Amplitude Spectra (FAS) of the ground motion at the surface and the FAS of the seismic input at the bedrock level.

The TTFs are shown in Fig. 3a together with the experimental SSR curves. It is worth noting that the SSR functions at stations MZ010 and MZ104 show anomalous trends likely related to instrument response factor removal before calculations of SSR, which suggested removing these functions from the following analyses. For more than half of the sites and in the frequency band of analysis (0.5-20 Hz), the 1D TTF do not show a satisfactory agreement with the experimental ones. Based on the visual inspection of Fig. 3a, some considerations can be done. As an example, both MZ09 and MZ01 sites are characterized by similar V_{S30} and share the same EC8 soil class B category (Felicetta et al. 2021). Despite not showing a similar trend of the SSR, the TTF of MZ09 has an average amplitude close to the experimental curve on a relatively wide frequency band, whereas the 1D modeling of MZ01 provides consistent response only for frequencies larger than 3 Hz. It is worthy of note that the Vs profile of MZ09 was derived using surface-wave passive array techniques which provide a significant velocity contrast at large depth (> 100 m), whereas the VS profile of MZ01 identifies the engineering bedrock at a shallow depth of about 28 m. MZ13 and MZ16 are both soft sites and the corresponding DH tests do not show a significant velocity contrast down to 20 and 50 m depth, respectively. On the other hand, the resonance frequencies are different (9 Hz vs 2 Hz), suggesting a seismic contrast at larger depth for MZ16 with respect to MZ13. This is confirmed by the 1D modeling, which is able to capture the experimental response with a closer agreement at MZ13 site, having a shallower velocity contrast.

Similar considerations may be made for the comparison between TTFs and EHVs (Figure 3b). In this case the EHVs of stations MZ010 and MZ104, which show no anomalies, were included in the following analyses.

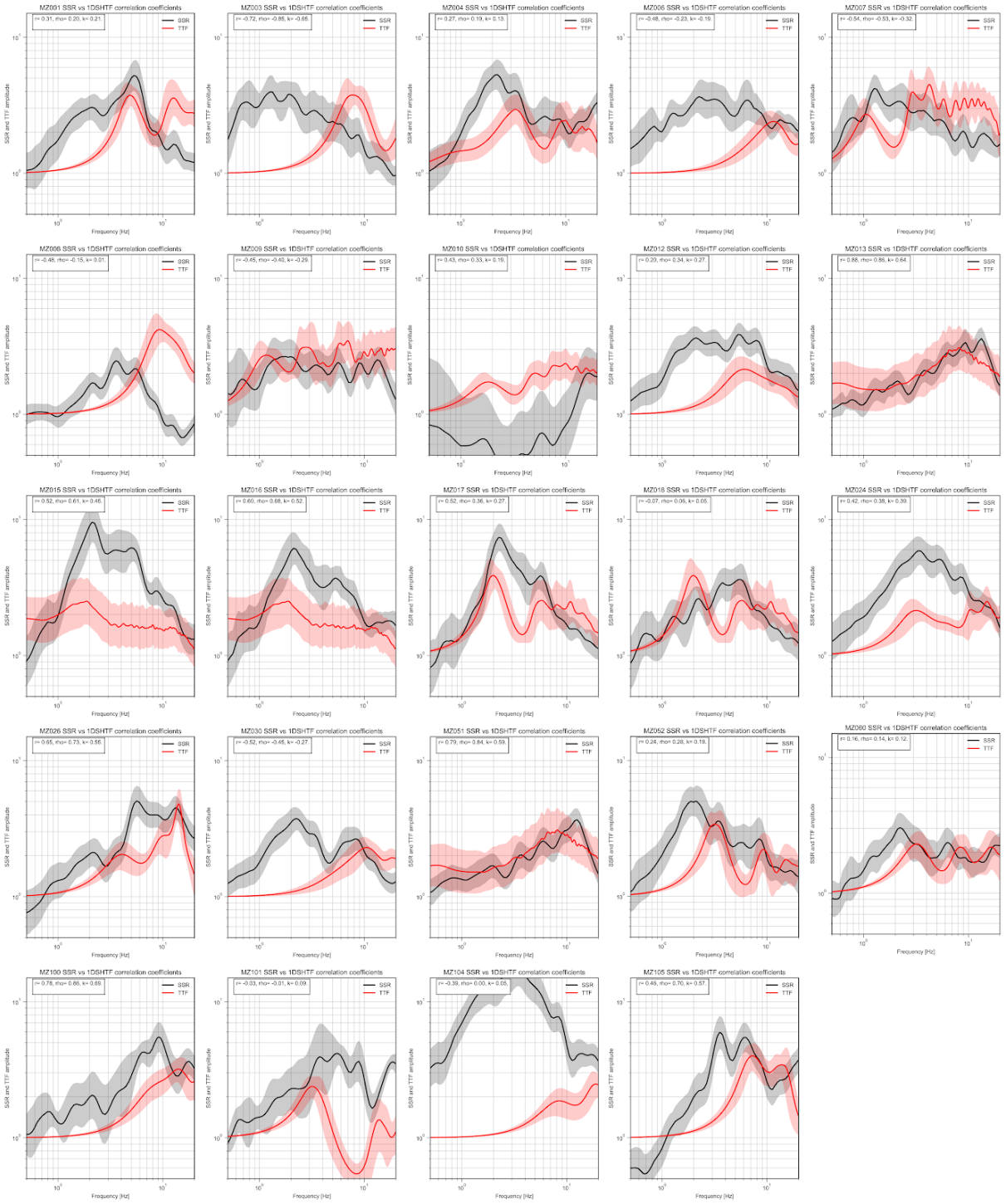

Figure 3a. Experimental SSR curves (black) versus theoretical 1D STRATA transfer functions (red) for 24 selected sites of the 3A network.

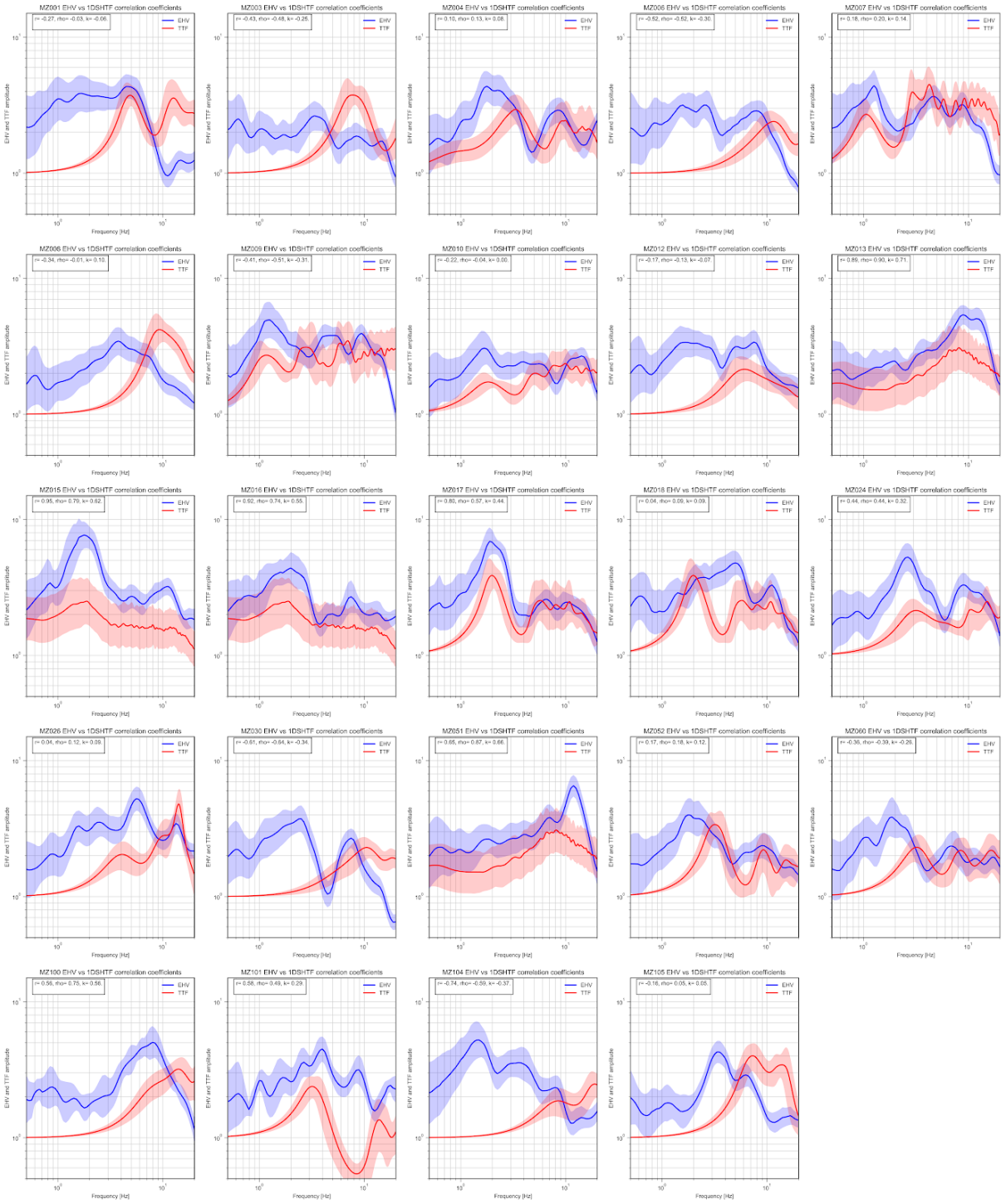

Figure 3b. Experimental EHV curves (blue) versus theoretical 1D STRATA transfer functions (red) for 24 selected sites of the 3A network.

Goodness-of-fit and applicability of 1D ground response analysis

Because we are interested in evaluating quantitatively the fit between the empirical and theoretical transfer functions, we apply taxonomy criteria for evaluating the site-specific applicability of the 1D approach in the site response analysis. In particular, we follow the strategies proposed in two recent papers by Thompson et al. (2012) and Tao and Rathje (2020).

Thompson et al. (2012) analyzed surface-to-borehole spectral ratio (SBSR) for some vertical Kik-net arrays in Japan and proposed to discriminate between 1D and not 1D sites computing two indicators: i) the inter-event variability of site response, and ii) the goodness-of-fit between ETF and TTF. The first indicator is defined as the median of the logarithmic standard deviations of the ETF (in this case equal to SBSRs). Indeed, the ETF variability in the frequency band of interest represents the uncertainties related to the dependence between site effects and source and path effects. The threshold value for this first indicator (σ hereinafter) suggested by Thompson is 0.35; sites with inter-event variability lower or higher the value of 0.35 are ranked as L and H, respectively. In our case, we select for the σ computation a frequency band of interest equal to 0.5-20 Hz, and the results are shown in Fig. 4 showing a predominance of low (L) inter-event variability sites. The second indicator proposed in the Thompson strategy is the fit between ETF and theoretical 1D SH model, aimed at searching the alignment of the resonant frequencies between experimental and theoretical curves in the frequency range where peaks of the ETFs are observed. The authors proposed to measure it with Pearson's sample correlation coefficient *r*, with a 0.6 threshold value discriminating between good (G) and poor (P) fit between experimental and theoretical curves. The classification of Thompson et al. (2012), given by the combination of σ and *r*, indicates finally four site categories: LG, LP, HP and HG.
LG sites (low inter-event variability and good fit between experimental and theoretical 1D resonances) are suitable for the 1D approach according to the authors. LP sites can be still appropriate for 1D ground response analysis, although some sources of misfit are present. HP and HG are sites where the 1D approach is not suitable.

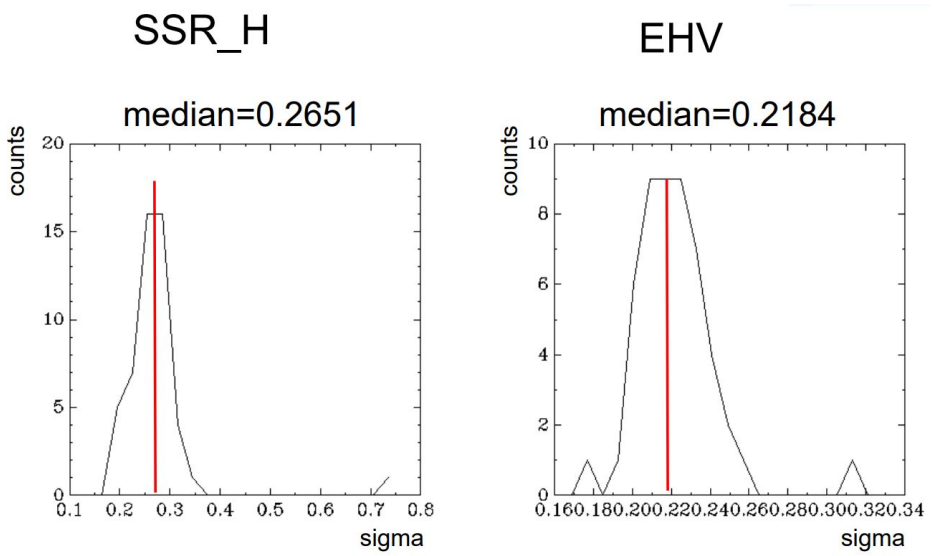

Figure 4. Inter-event variability (σ) computed following Thompson et al. 2012 for the standard spectral ratios computed on horizontal components (SSR_H), and for the earthquake horizontal-to-vertical ratios (EHV). The median computed on our data is also shown as the red line.

The second taxonomy strategy is described in Thao and Rathje (2020); they consider the H/V Spectral Ratio (EHV) computed on low-intensity earthquake data recorded by Kik-net vertical arrays as empirical transfer functions which are used to identify the resonant frequency ($f_{0,EHV}$) of the site (lower frequency peak in the EHV). They neglected goodness-of-fit metrics based on the computation of correlation coefficients. Because the database of Thao and Rathje is composed of downhole stations, their procedure pays attention to the pseudo-resonances generated from the effect of down-going waves (i.e waves traveling from the surface toward the position at the depth where seismic station is located). Pseudo-resonances are an artifact due to the fact that the receiver station is located not at the surface (outcrop) but at a certain depth (within). To discriminate between true (or outcrop) and pseudo-resonances (or within), these authors take into account the boundary conditions (outcrop or within) in the 1D modeling of TTFs. Thao and Rathje taxonomy is founded on the degree to which the

site is affected by pseudo-resonances and the alignment between the peaks of TTF (both _within and _outcrop) and ETF in the range where true resonances are present. These authors distinguished 4 site categories: for three of these (Groups A, B and C) the 1D approximation is suitable, whereas Group D contains sites for which the 1D assumption does not hold.
Group A is composed of true-resonance sites, which are characterized by a clear resonance peak in the EHV in the relatively low-frequency range ($f_{0,EHV}$ < 5 Hz) and good alignment between peak frequencies from EHV and TTF_within (ratio $f_{0,EHV}/f_{0,within}$ in the range of 0.8–1.2). Group B is composed by sites contaminated by pseudo-resonances, which are characterized by a clear resonance peak in the EHV in the relatively high frequency range ($f_{0,EHV}$ > 5 Hz) and good alignment between peak frequencies from EHV and TTF_outcrop ($f_{0,EHV}/f_{0,outcrop}$ in the range of 0.8–1.2). Group C distinguishes deep soil sites for which is not observable a strong seismic impedance contrast in the Vs profile; for such sites the EHV and TTF show a consistent flat shape. The non 1D sites, Group D, are characterized by i) having a clear peak in the EHV but a poor alignment between the peak frequency of the EHV and TTF (within and outcrop) or ii) showing no clear EHV peak but rather multiple low amplitude peaks with similar frequencies despite the presence of a significant seismic impedance contrast in the Vs profile. In this framework, it is fundamental the definition of clear EHV peak frequency, to this aim these authors proposed a simplified version of the SESAME criteria (Bard & SESAME Team, 2005).
As our dataset includes SSRs and EHVs as ETFs, which are unaffected by artifacts related to downgoing waves, we focused on the qualitative agreement between ETFs and TTF (calculated using outcropping boundary condition) in the case where ETFs have a flat shape, and on the alignment between peak frequencies of ETFs and TTFs (ratio of peak frequency in the range 0.8-1.2) in those cases where a clear peak is observed in the ETFs to distinguish between 1D and non 1D sites (akin Group D).
To summarize between the two taxonomy proposals, the strategy of Thompson et al. (2012) do not distinguish resonances and pseudo-resonances, and their classification is quantitative in nature and do not rely on the validity of the 1D assumption. Tao and Rathje (2020) assume that empirical EHV response is dominated by 1D site amplification (strong assumption), and do not take into account SSR, which are empirical transfer functions unaffected by pseudo resonances. Tao and Tathje (2020) do not use quantitative measures of goodness-of-fit metrics and do not consider the effect of amplification on the vertical component of motion. Although the taxonomy of Thao and Rathje was developed for downhole arrays to remove the boundary conditions, it can be used for any site (even non-downhole array sites) with an available Vs profile.

RESULTS AND DISCUSSION

To quantitatively measure the goodness-of-fit (GoF) between experimental curves (ETF) and theoretical STRATA 1D transfer functions (TTF), in addition to the Pearson's sample correlation *r* proposed by Thompson et al. (2012), we computed two additional parameters which do not imply linear relation between variables (Table 1): the Spearman's rank correlation coefficient ρ and Kendall's tau correlation coefficient τ (Zhu et al. 2020). All the three coefficients, computed in the frequency range 1.0-15 Hz, range from -1 (total negative correlation) to 1 (positive correlation). In literature (Pilz and Cotton 2019; Felicetta et al. 2021), a threshold correlation value of 0.6 is generally set to classify sites with a ''good" (G) or "poor" (P) fit. Figure 5 shows the three correlation parameters for our stations indicating a similar trend among *r*, *ρ* and τ. Despite almost all sites can be considered as low inter-event variability sites (L), only very few stations are characterized by a correlation higher than 0.6: 2/22 stations in case of τ and 7/22 stations in case of ρ measured between SSR and TTF (Figure 5, left panel); 3/24 stations in case of τ and 5/24 stations in the in case of ρ and *r* measured between EHV and TTF (Figure 5, right panel).
Therefore, in the best case, barely about 32% of sites can be classified as LG for which the 1D assumption is suitable. The values of the three correlations are reported in Table 1 for the selected stations, together with other information (such as fundamental frequency f_0) useful for applying the Gof metrics evaluating the agreement between TTF and ETF. The classification of sites using

Thompson et al. (2012) criteria and the cluster groups, as found by Felicetta et al. (2021) for the horizontal (CH) and vertical (CV) components, are also reported in Table 1.

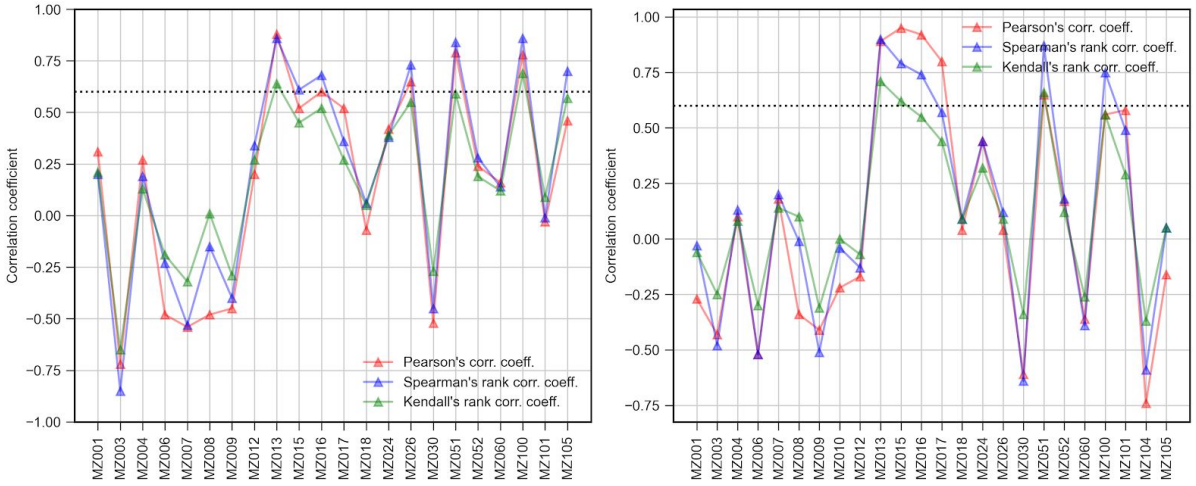

Figure 5. Correlation between experimental SSR (left panel) and EHV (right panel) curves and theoretical 1D STRATA transfer functions: Pearson's sample correlation coefficient (red), Spearman's rank (black) and Kendall's correlation (blue). The dashed line indicates the 0.6 threshold level.

In terms of the classification proposed by Tao and Rathje (2020), for those stations showing a clear peak in the ETFs, we measured the agreement of peak frequency between ETF and TTF by their ratios. The distinction of clear ETF peaks is based on the use of the following criteria suggested by SESAME (Bard & SESAME Team, 2005): i) amplitude of the ETF at peak frequency $A_0 > 2$; ii) standard deviation of the ETF < 2; iii) amplitude of the ETF < $A_0/2$ in at least one of two the intervals [$f_0/4$; f_0] and [f_0, f_0*4]; iv) standard deviation of the ETF at the peak frequency < theta, which is a frequency dependent threshold.

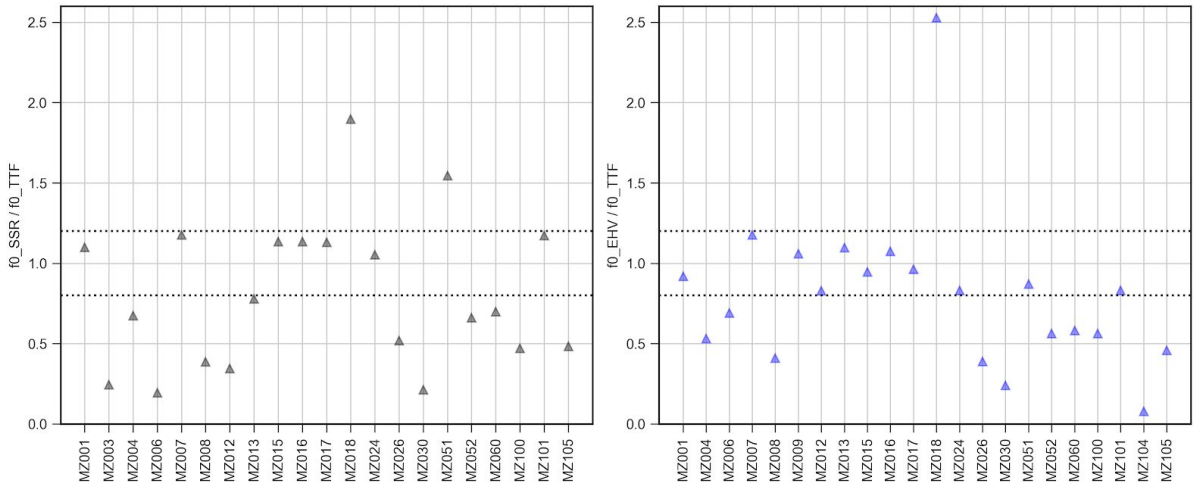

Figure 6. Ratio between f_0 measured on the SSR and peak frequency of the TTF (right panel) for those stations exhibiting a clear peak. Ratio between f_0 measured on the EHV and peak frequency of the TTF (left panel) for those stations exhibiting a clear peak. The dashed lines indicate the 0.8 and 1.2 threshold level.

In the case of SSRs, for those stations exhibiting a clear peak (21/22), only for 33% we found a satisfactory agreement with the fundamental frequency of TTF (f_0 ratio within about +/-20%, Fig. 6-left panel). In the case of MZ009, the SSR and TTF show multiple low-amplitude peaks which do not satisfy the adopted criteria for a clear peak recognition (Fig. 3a).
In the case of EHVs, 22 stations show a clear peak and we found a satisfactory agreement with the fundamental frequency of TTF in about 50% of the stations (Figure 6-right panel). In one case, MZ003, the EHV shows multiple low-amplitude peaks whereas the TTF has a clear peak at about 7.8 Hz (Fig. 3b). In another case, MZ010, the TTF shows no clear peak whereas the EHV has a clear peak at about 1.7 Hz.
Overall, the Tao and Rathje (2020) classification relaxes the criteria for the suitability of the 1D assumption applied to ground response analysis with respect to the Thompson et al (2012), and the number of suitable sites increases from 30% to about 50% considering the most favourable parameters, namely the evaluation of the peak alignment between EHV and TTF. However, it shall be noticed that, as the SSR represents the more robust estimator of site amplification, a satisfactory alignment of resonance peaks between SSR and TTF is retrieved only for about 32% of sites.
The comparison between the experimental amplification functions and the 1D theoretical site amplification (Fig.s 3 and 6, and Table 1) show that for the majority of sites there is no general agreement between experimental and numerical estimates, also in the linear-elastic condition. Considering the ETF as the benchmark for site response estimation, the almost systematic bias in the numerical site response may be explained by two main factors: i) a large part of the 3A sites is located in geological-geomorphological conditions which violate the 1D seismic wave propagation assumption, and ii) even in those cases where the 1D wave propagation assumption may be considered fulfilled, the available subsurface characterization is too shallow and not sufficient to investigate the seismic impedance contrast responsible for the observed seismic amplification. Recently, several studies on recordings obtained by vertical arrays with available detailed subsurface characterization have proved that 2D/3D site effects are commonly found on data recorded at the surface (Pilz & Cotton; 2019). For the 3A network, the morphology of sites is described by steep slopes, valley floors and terrace edges (Felicetta et al 2021), and all these conditions suggest that 2D and 3D seismic-wave propagation shall be adopted in order to correctly evaluate site response. In addition to 2D/3D effect, for the 3A network sites, the investigation depth of DH tests is generally within the shallower 30 m. Only in a few cases the investigation depth reaches 50 m. Where the experimental site amplification shows f_0 in the low frequency range (below 2 Hz), considering the associated wavelength (in the order of 100 m), the investigation depth may not be sufficient to reach the main seismic impedance contrast responsible for the peak observed in the amplification function. In such cases, the use of 2D passive seismic arrays may provide useful information for deriving deep Vs profiles to be used in theoretical site response analysis. Further, our 1D simulations are based on Vs profiles not directly obtained at the recording site mainly due to logistic reasons at the time of downhole or geophysical surveys (maximum distance of the order of 100 m). This also may bias our analysis. As on-going work, we are inverting directly the HVSR curves (i.e the spectral ratios from noise data) using the diffuse field approach (DFA) in order to compare theoretical and experimental HVSRs. A good fit could ensure that the available Vs profile obtained from DH or geophysics tests is representative of the investigated site. If not, the geophysical surveys were likely too distant from the stations and not representative of the investigated site. In this latter case, our aim is to adopt the Vs model derived from the DFA inversion and investigate if the inverted model improves the fit between SSR and newly calculated TTF.

Table 1. For each selected station we list the values of: the Spearman's correlation coefficients calculated between SSR and TTF (ρ) and between EHV and TTF (ρ*); the fundamental resonance (f_0) from EHV curves, from SSR curves and theoretical 1D models; the Thompson rank; and the cluster analysis as computed in Felicetta et al. (2021). The grey cells indicate correlation values higher than 0.6.

Station name	ρ	ρ^*	$f0_{\_EHV}$ (Hz)	$f0_{\_SSR}$ (Hz)	$f0_{\_TTF}$ (Hz)	rank	Cluster
MZ001	0.20	-0.03	4.46	5.36	4.89	LP	CH1 CV1
MZ003	-0.85	-0.48	-	1.90	7.77	LP	CH2 CV2
MZ004	0.19	0.13	1.76	2.23	3.31	LP	CH3 CV2
MZ006	-0.23	-0.52	7.92	2.24	11.47	LP	CH2 CV1
MZ007	-0.53	0.20	1.26	1.26	1.07	LP	CH2 CV2
MZ008	-0.15	-0.01	3.77	3.57	9.18	LP	CH4 CV3
MZ009	-0.40	-0.51	1.24	-	1.17	LP	CH5 CV3
MZ010	-	-0.04	1.67	-	-	-	?? ??
MZ012	0.34	-0.13	5.07	2.11	6.11	LP	CH1 CV2
MZ013	0.86	0.90	8.85	6.28	8.06	LG	CH5 CV3
MZ015	0.61	0.79	1.76	2.12	1.86	LG	CH3 CV2
MZ016	0.68	0.74	2.00	2.12	1.86	LG	CH3 CV2
MZ017	0.36	0.57	1.90	2.23	1.97	LP	CH3 CV2
MZ018	0.06	0.09	4.98	3.74	1.97	LP	CH1 CV3
MZ024	0.38	0.44	2.65	3.36	3.19	LP	CH3 CV2
MZ026	0.73	0.12	1.58	2.11	4.06	LG	CH5 CV1
MZ030	-0.45	-0.64	2.51	2.23	10.45	LP	CH2 CV1
MZ051	0.84	0.87	7.08	12.57	8.13	LG	CH5 CV3
MZ052	0.28	0.18	1.80	2.11	3.19	LP	CH3 CV3
MZ060	0.14	-0.39	1.86	2.23	3.19	LP	CH2 CV1
MZ100	0.86	0.75	7.92	6.63	14.06	HG	CH5 CV1
MZ101	-0.01	0.49	2.65	3.74	3.19	LP	CH1 CV1
MZ104	-	-0.59	1.49	-	18.92	LP	?? ??
MZ105	0.70	0.05	3.37	3.55	7.35	LG	CH1 CV1

REFERENCES

Bard, P.-Y. and SESAME Team (2005). "Guidelines for the implementation of the H/V spectral ratio technique on ambient vibrations measurements, processing and interpretation", *Deliverable D23.12 of the SESAME project*, 62 pp.

Cara, F., Cultrera, G., Riccio, G. et al. (2019). "Temporary dense seismic network during the 2016 Central Italy seismic emergency for microzonation studies", *Sci Data*, **6**(182), https://doi.org/10.1038/s41597-019-0188-1.

Felicetta, C., Mascandola, C., Spallarossa, D., Pacor, F., Hailemikael, S. and Di Giulio, G. (2021). "Quantification of site effects in the Amatrice area (Central Italy): Insights from ground-motion recordings of the 2016–2017 seismic sequence", *Soil Dynamics and Earthquake Engineering*, **142**, https://doi.org/10.1016/j.soildyn.2020.106565.

Kottke, A. R., and E. M. Rathje, (2009). "Technical manual for Strata", Report No.: 2008/10. Pacific Earthquake Engineering Research Center, University of California, Berkeley.

Milana, G., Cultrera, G., Bordoni, P., Bucci, A., Cara, F., Cogliano, R., Di Giulio, G., Di Naccio, D., Famiani, D., Fodarella, A. and Mercuri, A., (2019), "Local site effects estimation at Amatrice (Central Italy) through seismological methods". *Bulletin of Earthquake Engineering*, pp.1-27.

Luzi L., Lanzano G., Felicetta C., D'Amico M. C., Russo E., Sgobba S., Pacor, F., & ORFEUS Working Group 5 (2020). "Engineering Strong Motion Database (ESM) (Version 2.0)", Istituto Nazionale di Geofisica e Vulcanologia (INGV). https://doi.org/10.13127/ESM.2.

Pilz, M., and F. Cotton, (2019). "Does the one-dimensional assumption hold for site response analysis? A study of seismic site responses and implication for ground motion assessment using KiK-Net strong-motion data". *Earthquake Spectra*, **35**(2), pp.883-905.

Spearman C. (1904). "The proof and measurement of association between two things", *Am J Psychol,* **15**, 72–101.

Tao, Y. and Rathje, E., (2020). "Taxonomy for evaluating the site-specific applicability of one-dimensional ground response analysis", *Soil Dynamics and Earthquake Engineering*, **128**, p.105865.

Thompson, E.M., Baise, L.G., Tanaka, Y. and Kayen, R.E., (2012). "A taxonomy of site response complexity", *Soil Dynamics and Earthquake Engineering*, **41**, pp.32-43.

Toro, G.R., (1995). "Probabilistic models of site velocity profiles for generic and site-specific ground-motion amplification studies", Technical Report 779574, Brookhaven National Laboratory, Upton, NY.

Zhu, C., Pilz, M. and Cotton, F., (2020). "Evaluation of a novel application of earthquake HVSR in site-specific amplification estimation", *Soil Dynamics and Earthquake Engineering*, **139**, p.106301.